

NASA TECHNICAL NOTE



NASA TN D-3623

C.1

NASA TN D-3623

LC 111 00716 R 11
11 11 11 11 11
KIRTLAND AFB,



**INTERPLANETARY MIDCOURSE GUIDANCE
USING RADAR TRACKING AND
ON-BOARD OBSERVATION DATA**

by Luigi S. Cicolani
Ames Research Center
Moffett Field, Calif.

TECH LIBRARY KAFB, NM



0130319

INTERPLANETARY MIDCOURSE GUIDANCE USING RADAR TRACKING
AND ON-BOARD OBSERVATION DATA

By Luigi S. Cicolani

Ames Research Center
Moffett Field, Calif.

NATIONAL AERONAUTICS AND SPACE ADMINISTRATION

For sale by the Clearinghouse for Federal Scientific and Technical Information
Springfield, Virginia 22151 - Price \$2.00

TABLE OF CONTENTS

	Page
SUMMARY	1
INTRODUCTION	1
SYMBOLS	2
ANALYSIS	4
Simulation of the Interplanetary Guidance and Navigation Problem . . .	4
Reference trajectories	4
Injection and velocity-correction errors	5
Filtering of Measurements	5
On-board observations	6
Radar observations	6
Velocity-correction measurement	7
Velocity-correction schedule	7
RESULTS AND DISCUSSION	9
Observation Schedules	9
High-speed mission, Earth-Mars leg	9
High-speed mission, return leg	11
Venus swing-by mission, Earth-Mars leg	11
Venus swing-by mission, Mars-Venus leg	11
Venus swing-by mission, Venus-Earth leg	12
Comparison With Performance Predicted by the Optimum Correction- Schedule Theory	12
Comparison With Performance of the On-Board Navigation System	13
CONCLUDING REMARKS	14
APPENDIX A.- DERIVATION OF OPTIMUM VELOCITY-CORRECTION SCHEDULE	16
General Problem	16
Velocity corrections	16
The miss vector	17
Statistical properties	17
Problem of the optimum correction schedule	18
Simplifying Assumptions	19
Independence of correction and observation schedules	19
Simplified correction-error model	20
Approximation of V_j	21
Approximation of $A_2(t_F, t)$	21
Simplified Problem and Its Solution	22
Optimum correction schedule for the simplified problem	22
Computation of t_1	24
Number of corrections	24
Off-optimum timing	25
REFERENCES	27
TABLE I.- REFERENCE TRAJECTORY PARAMETERS	28

TABLE II.- RMS INJECTION, CORRECTION, AND MEASUREMENT ERRORS	29
TABLE III.- NAVIGATION SCHEDULE	30
TABLE IV.- COMPARISON WITH PREDICTED PERFORMANCE (RMS)	35
TABLE V.- COMPARISON WITH PREDICTED PERFORMANCE - VENUS WING -BY MISSION	36
TABLE VI.- COMPARISON OF PERFORMANCE WITH ON-BOARD SYSTEM	37
FIGURES	39

INTERPLANETARY MIDCOURSE GUIDANCE USING RADAR TRACKING
AND ON-BOARD OBSERVATION DATA

By Luigi S. Cicolani
Ames Research Center

SUMMARY

This paper examines the performance of midcourse guidance and navigation systems for manned interplanetary missions when radar range and range-rate measurements and on-board theodolite observations are available as sources of navigation data. Results are given for two Mars missions, one a direct flight to Mars and back and the other a round trip with return via Venus.

Reasonable observation schedules to refine the miss estimate to the accuracy required for entry or close approach are found to consist primarily of radar observations for estimating the greatest part of the miss, plus frequent on-board observations of the target planet during the approach to Mars or Venus, or radar observations during the approach to the Earth. Additional on-board observations during the departure from distant planets are usually helpful in reducing fuel requirements.

The system performance is such that the miss is generally estimated better than it can be controlled. Consequently, the work of Lawden can be applied to obtain an analytical solution for the a priori optimum correction schedule. The minimum fuel requirements, the correction size, and the dependence of these parameters on the number of midcourse corrections are also determined by the theory. Results of optimum four-correction schedules used in the simulations on all legs of the two missions agree fairly well with the theory.

The velocity-correction requirements for the various legs range from 18 to 24 m/sec, and the rms miss in pericenter radius at arrival is less than 2.8 km at Earth and Mars and 6 km at Venus. The downrange miss varies from 2 to 22 km.

INTRODUCTION

In manned interplanetary missions the advantages of a self-contained on-board midcourse guidance and navigation system independent of communications with Earth are evident. The performance of such systems is discussed in reference 1, where it is found that navigation for the entire mission can be carried out reasonably well with only the on-board system.

Nevertheless, communications will normally be operational and both ground-based radar tracking and on-board observations will be available as navigation data sources. Ground tracking is usually superior to on-board observations in estimating the trajectory, but its ability to establish the

relative motion to the accuracy desired for manned missions during the approach to distant planets is limited. Consequently, the present study was initiated to evaluate the performance possible from the use of both tracking and on-board observational data.

Midcourse guidance and navigation refers to the process of estimating and controlling the terminal miss at the target planet. This is carried out by a sequence of observations and trajectory corrections. To determine system performance it is necessary, first, to obtain appropriate observation and correction schedules. The observation schedules are determined empirically to utilize the more effective observation type or combination of types in each region of the mission; sufficient observations are made to determine system performance near the limit of its capability. The correction schedule should be selected to minimize the fuel requirements and, in this study, a good approximation to the optimum correction schedule is obtained analytically using the method of Lawden (ref. 2).

The discussion of system performance considers the accuracy of the miss estimation, the terminal miss, and the velocity correction requirements. Results are given from simulation of the system for two reference missions; both are round-trip missions to Mars, one a direct trip and the other includes a swing past Venus during the return to Earth. The trajectory estimation is based on the Kalman filter theory and the results are given in terms of the standard deviations of the random variables of interest.

SYMBOLS

$A(t_2, t_1)$	transition matrix relating the deviation state at t_2 to the deviation at t_1
$A_j(t_2, t_1)$	$j = 1, \dots, 4$, submatrices of $A(t_2, t_1)$
$B(t_F, t)$	matrix relating miss to current state deviation
C	covariance matrix, commanded velocity correction
$\overline{c^2}$	trace (C)
e	measurement error
$H(t)$	matrix relating observable to current state deviation
I	unit matrix
K	weighting matrix
$M(t)$	covariance matrix, miss
$m(t)$	miss

m_a rms allowable terminal miss
 N number of midcourse velocity corrections
 $P(t)$ covariance matrix, current uncertainty in state estimate
 $PAR(t)$ covariance matrix, current state deviation
 Q covariance matrix, measurement error
 r range
 \dot{r} range rate
 S covariance matrix, velocity-correction error
 T sum of rms midcourse velocity corrections
 t time
 t_F reference arrival time
 t_j time of j th midcourse velocity correction
 $\bar{u}_r, \bar{u}, \bar{p}, \bar{n}$ unit vectors, defined where used
 V covariance matrix, velocity correction
 ΔV velocity correction
 $x(t)$ current state deviation from reference state
 y measured value of observable
 $\overline{\gamma^2}$ variance, aiming error in velocity correction
 $\delta()$ small deviation from reference value of ()
 $\overline{\epsilon^2}$ variance, cutoff error in velocity correction
 $\overline{\kappa^2}$ variance, proportional error in velocity correction
 σ_r standard deviation, error in radar range measurement
 $\sigma_{\dot{r}}$ standard deviation, error in radar range-rate measurement
 $()^T$ transpose of ()
 (\sim) error in estimate of ()
 $(\hat{ })$ estimate of ()

- ()₀ value of () at injection
- ()_F value of () at t_F
- ($\bar{\quad}$) expected value of ()
- ()_p quantities at pericenter

ANALYSIS

The performance of the midcourse guidance and navigation system is evaluated by simulating its operation. The detailed analysis of this simulation has been discussed extensively in reference 1 and the reports it cites; thus, only a brief review of the pertinent background is necessary here.

Simulation of the Interplanetary Guidance and Navigation Problem

The following process is to be simulated. A vehicle is injected onto a reference interplanetary orbit, that is, one with desired end conditions. Because of random injection errors, the reference orbit is not obtained and the guidance and navigation system must estimate and control the end conditions. The estimation is carried out by processing observation data. In this study the data are obtained from on-board theodolite observations of various planets and Earth-based radar range and range-rate measurements. These observations are subject to random measurement errors and their processing is based on the Kalman filter theory. Several times during the flight, impulsive velocity corrections are made to control the end conditions. These corrections are determined by means of a guidance law from the estimated end conditions, and are subject to random execution errors.

In the mathematical analysis of this process two assumptions are made: (1) all input random variables (injection, correction, and measurement errors) are gaussian distributed with zero means, and (2) the orbits of interest are sufficiently near the reference orbit to allow linearization of the equations of motion. Consequently, the output random variables (velocity corrections, terminal miss, miss estimate uncertainty, vehicle state, etc.) are linear combinations of the input random variables and, therefore, are gaussian distributed with zero means. Thus, the simulation need consider only the covariance matrices of the various quantities of interest.

Reference trajectories.- Two round-trip manned Mars mission trajectories, including a stopover on Mars, are used as reference trajectories. Both are taken from reference 1 where they are referred to as the high-speed mission and the Venus swing-by mission. A brief list of orbital parameters is given in table I. Reference 1 also gives projections of these trajectories and of the planetary orbits on the ecliptic plane, which are useful in visualizing the relative position of the vehicle and planets at various times in the mission.

Injection and velocity-correction errors.- The injection errors of reference 1 are assumed here and are listed in table II. The errors are assumed to be identical at both Earth and Mars injections and also are identical to the initial uncertainty in the estimate of the state. The miss and miss uncertainty at the start of the Venus-Earth leg of the Venus swing-by mission are also listed in table II. These are, of course, obtained from a particular simulation of the preceding Mars-Venus leg.

For velocity-correction errors, the model of reference 1, appendix B, has been adopted. Briefly, it includes proportional, aiming, and cutoff errors, and has the following covariance matrix for the correction error:

$$S = \overline{\kappa^2}C + \frac{\overline{\gamma^2}}{2} (\overline{c^2}I - C) + \overline{\epsilon^2} \frac{C}{\overline{c^2}}$$

where C is the covariance matrix of the commanded velocity correction and $\overline{c^2}$ its trace. The values of $\overline{\kappa^2}$, $\overline{\gamma^2}$, and $\overline{\epsilon^2}$ (variances of the proportional, aiming, and cutoff errors) are listed in table II.

Each midcourse velocity correction attempts to null the miss as computed from the estimated state. Fixed time-of-arrival (FTA) guidance (see ref. 1 for the corresponding expression for C) will be used throughout. Miss for FTA guidance is defined as the position deviation at the reference arrival time, which corresponds to pericenter on the reference orbit.

Filtering of Measurements

All navigation information is assumed to be processed by a Kalman filter. Let $P(t)$ be the covariance matrix of the uncertainty in the estimated current deviation state. Suppose the measurement is

$$y = Hx + e$$

where y is the measured value of the observable, Hx is the true value of the observable, and e is the random error in the measurement. The H matrix consists of partial derivatives of the observables with respect to the state variables. After an observation, the new uncertainty covariance matrix is

$$P' = (I - KH)P$$

where K is the filter weighting matrix

$$K = PH^T(Q + HPH^T)^{-1}$$

and

$$Q = \overline{(ee^T)}$$

On-board observations.- A number of on-board optical observations can be considered, for example, planet diameter, sextant, and theodolite measurements. Reference 1 indicates that planet diameter measurements are inferior and that, while the sextant is more convenient to operate than the theodolite, a sufficient number of sextant observations with suitably chosen stars will give results equivalent to those obtained from the theodolite. For these reasons and for computational simplicity, the on-board measurements of this study are restricted to theodolite observations.

The theodolite measures the celestial latitude and longitude of the observed body and thereby determines the vehicle's position deviation normal to the line of sight to the planet. Its H matrix and error model are discussed in reference 1. The resulting covariance matrix of measurement errors is, from reference 1, the diagonal 2×2 matrix:

$$Q = \left(\overline{q^2}_{inst} + \overline{b^2} \theta^2 + \frac{\overline{\delta R_s^2}}{R^2} \right) I$$

where θ is the half subtended angle and R is the distance to the observed body. The quantities q_{inst} , b , and δR_s are the random instrument error, planet radius uncertainty, and planet position uncertainty, respectively. Their rms values are listed in table II.

Radar observations.- A network of three stations (Goldstone, Johannesburg, and Woomera) was assumed with the viewing station measuring range and range rate simultaneously. The (2×6) H matrix for these measurements is

$$H^T = \begin{bmatrix} \bar{u}_r & \left(I - \bar{u}_r \bar{u}_r^T \right) \frac{\bar{v}_v/s}{r} \\ \bar{o} & \bar{u}_r \end{bmatrix}$$

where \bar{u}_r is a unit vector in the direction of the line of sight from the station to the vehicle, \bar{v}_v/s is the velocity of the vehicle relative to the viewing station, and r is the range. All quantities are evaluated on the reference orbit. The two columns of H^T are the derivatives of range and range rate, respectively, with respect to the state variables.

Radar measurements are affected by a variety of errors from various sources including white noise, colored noise (noise with finite correlation time), bias errors from the radar equipment, and errors from other sources, such as, station location, station clock, and astronomical unit uncertainties. A comprehensive list of such errors in a study of guidance and navigation in the lunar mission is considered in reference 3. For simplicity, the present study considers only white-noise errors. The variances of these errors for the range and range-rate measurements are given below. These were obtained from reference 3 by combining the white- and colored-noise variances listed there. This is approximately valid because the time constant of the colored noise is short compared to time between observations.

$$\text{Range: } \sigma_r^2 = a_0^2 + a_1^2 r^2 \quad (\text{km}^2)$$

$$\text{Range rate: } \sigma_{\dot{r}}^2 = b_0^2 + b_1 \varphi^2 r^2 + b_2 \varphi^2 r + b_3 \varphi^4 \quad (\text{m/sec})^2$$

where

$$\varphi = 1 + 0.03 \dot{r} \quad b_1 = 2 \times 10^{-13}$$

$$a_0 = 0.00525 \quad b_2 = 6.5 \times 10^{-8}$$

$$a_1 = 0.767 \times 10^{-7} \quad b_3 = 2 \times 10^{-4}$$

$$b_0 = 0.1$$

In these expressions the dimensions of r and \dot{r} are km and km/sec, respectively.

The rms range measurement error increases almost linearly with range outside the Earth's sphere of influence (fig. 1).

The range-rate measurement error depends on both the range and range rate. As an example, the time history of the rms range-rate error for the outbound leg of the high-speed mission is plotted in figure 2.

Velocity-correction measurement. - Accurate accelerometers are assumed to be on board the vehicle for measuring the executed velocity corrections. The accelerometer measurement errors are assumed equally likely in all directions with an rms value of 1 cm/sec.

Velocity-Correction Schedule

With the use of radar the question of an optimum velocity-correction schedule can be settled analytically from the work of Lawden (ref. 2). The application of his work to the present problem is discussed in detail in appendix A, and a brief description of the solution is given below.

The analytical solution is based on three assumptions:

1. At the time of each correction the miss has been estimated better than it can be corrected.
2. The terminal miss due to current velocity deviations is proportional to the time to go.
3. The miss generated by random errors in each correction is principally caused by the cutoff error.

The first assumption leads to a velocity-correction schedule independent of the observation schedule; consequently, the first correction cancels almost all the miss due to injection errors, and subsequent corrections account principally for the miss generated by random errors in the preceding correction. The problem then becomes mathematically tractable as a result of the second

and third assumptions. In the solution, the optimum timing of each correction represents a compromise between the fuel cost for subsequent corrections, which decreases with a delay of the current correction because the post-correction miss is reduced, and the fuel cost of the current correction, which increases with a delay.

In the current simulations the three assumptions are generally satisfied. In all the trajectories examined here, radar observations are sufficiently effective in estimating the orbit (compared to the errors in correcting it) that the first condition is generally satisfied. The second assumption requires that the matrix $A_2(t_F, t)$ (a submatrix from the state transition matrix which relates position deviations at t_F to velocity deviations at t) be proportional to the time to go, $t_F - t$. For typical interplanetary orbits, this assumption is satisfied for $t_F - t$ corresponding to somewhat less than half an orbit. This assumption is commonly violated in the early phase of an interplanetary orbit. However, no difficulty arises because the optimum timing of the first correction is determined empirically and, therefore, none of the three assumptions need be met for the first correction. The remaining corrections will usually occur much later in the flight, more than halfway to the target position, where the optimum scheduling of corrections can be obtained analytically.

The third assumption will be valid, for the present error model, for midcourse correction magnitudes to 5 m/sec. All but the first correction will usually fall within this range. Again, this presents no difficulty since the timing of the first correction will be empirically determined.

If the three assumptions are satisfied, the optimum correction schedule is obtained as follows: Assuming there are N corrections, the optimum timing of the j th correction is

$$t_F - t_j = \frac{m_1}{\sqrt{\epsilon^2}} \left(\frac{m_a}{m_1} \right)^{\frac{j-1}{N-1}} \quad j = 2, \dots, N$$

where m_a is the allowable rms terminal miss and m_1 is the miss uncertainty after the first correction. The timing of the first correction is determined empirically such that the sum of the rms corrections

$$T = \sum_{j=1}^N c_j = c_1(t_1) + (N - 1) \sqrt{\epsilon^2} \left[\frac{m_1(t_1)}{m_a} \right]^{\frac{1}{N-1}}$$

is a minimum.

Lawden (ref. 2) reports an optimum number of corrections, N^* , which give the least value of T . The value of N^* is typically between 8 and 10. However, the present work will usually use a four-correction schedule since for a larger number of corrections the individual corrections become small, of the order of the errors in making corrections, and the time interval between the last few corrections also becomes small. Appendix A indicates that there is little fuel penalty for using four or five corrections rather than the optimum number.

RESULTS AND DISCUSSION

The following discussion considers the nature of reasonable observation schedules for the combined use of radar and on-board observations, and compares the resulting performance with that theoretically predicted for the optimum correction schedule and with the performance of the purely on-board system of reference 1.

Observation Schedules

The observation schedules are determined empirically. A schedule is sought that satisfies the condition that the miss can be better estimated than it can be corrected at the time of each correction. When this goal is approached, the fuel requirements will be near the minimum and the terminal miss performance can then be improved somewhat by increases in the number of observations. The initial choice of schedule and further adjustments to this schedule need not be made arbitrarily; past studies, such as references 1 and 3, have already indicated that radar provides superior information in most regions of the missions and that on-board observations are most effective during approach and passage near the planets. Thus, an initial schedule might consist entirely of radar measurements. The number of measurements is then increased, and on-board observations are added and increased where effective until further adjustments show very little improvement in performance.

More organized empirical approaches, such as the method of steepest descent employed in reference 4, can be used to generate the most economical schedule. However, economical schedules are not of interest here since ground tracking normally generates and processes data in large quantities. Rather, this study seeks sample schedules which demonstrate the performance possible when both on-board observational and radar-tracking data are used.

Observation schedules for each leg of both reference missions are discussed below. The observation and correction schedules are listed in table III, and the corresponding time histories of rms miss uncertainty are plotted in figures 3 and 4. It should be noted that, although these curves are drawn smoothly, the rms miss uncertainty is a decreasing step function with step changes occurring at each observation. In addition, accelerometer measurement errors introduce a comparatively minute step increase in rms miss uncertainty at the time of each correction, although this effect is usually not visible at the scale of the figures.

High-speed mission, Earth-Mars leg. - The reference trajectory for this case is type I (trajectories will be classed as type I if the total heliocentric angle from injection to arrival is less than 180° , and type II otherwise) with a total flight time of 112.5 days.

The navigation schedule (table III(a)) and the resulting time history of the miss uncertainty (fig. 3(a)) show that a modest number of radar observations can rapidly reduce the miss uncertainty to several hundred kilometers. This accuracy will satisfy the minimum fuel condition until the second

midcourse correction; therefore, no observations are made during most of the heliocentric phase of the flight. During the approach to Mars, radar observations alone are inadequate; however, frequent theodolite observations give a sufficiently accurate determination of the miss.

The range-rate measurements provide very little information on the miss due to the large measurement errors postulated. Simulation without range-rate measurements (results not shown) shows virtually the same performance as that obtained for the system with both range and range rate. Thus, the performance obtained here for the radar system would apply as well if only range measurements were made. Similar remarks apply to the remaining legs of the two missions.

The approach-phase schedule can be examined in greater detail to illustrate the capabilities of on-board and radar measurements in this region. The approach phase refers to the 3-day interval from 109.3 to 112.32 days which includes the last two velocity corrections and ends at the final correction. For the reference navigation schedule, the rms miss uncertainty at the beginning of the approach phase is 36.6 km, which, after 42 theodolite observations of Mars, reduces to 4.9 km.

The capabilities of theodolite observations during the approach phase are illustrated in figure 5. The data show the variation in the downrange, crossrange, and radial components of the terminal miss uncertainty for (1) different numbers of observations in the approach phase, and (2) three initial levels of miss uncertainty. The approach-phase schedules used here consist of a sequence of theodolite observations with twice as many between the third and fourth corrections as in the segment prior to the third correction. In each case the observation rate is uniform in each of the two segments of the approach phase. The minimum number of observations considered is 12 and the maximum 99, and the corresponding maximum observation rate is once each half hour. The three levels of initial miss uncertainty resulted from the omission of various blocks of observations from the reference schedule prior to the approach phase.

Two fundamental differences are seen between the estimation of the downrange component of miss uncertainty and the crossrange and radial components. First, the performance in the downrange component is dependent upon and approximately proportional to the initial uncertainty; whereas, in the other components, performance is independent of the initial values. Second, the minimum number of observations gives nearly as good results for the downrange component as the maximum number, while in the radial and crossrange components performance is significantly improved when the number of observations is increased. This suggests an inherent limit on the ability of theodolite observations in this interval to resolve the downrange component of miss.

To obtain comparable data on the usefulness of radar data during the approach phase, additional simulations were run (results not shown) which indicated that even very accurate radar observations in the approach phase (1 km in range and 0.5 m/sec in range rate) cannot reduce the downrange, crossrange, and radial components of terminal miss uncertainty much below the

initial values. Apparently, for the particular reference trajectory used here, none of these components of miss uncertainty correspond very closely to that component which can be resolved by radar data.

High-speed mission, return leg.- The reference trajectory is type II with a flight time of 190.77 days.

With radar (table III(b), fig. 3(b)) no on-board observations are necessary. The schedule consists of radar measurements at 4-day intervals until the first correction and at 10-day intervals thereafter until the last 15 days of the flight when more frequent observations are made. Relatively few observations were required during the entire flight.

It may be noted that observations of Mars during departure from that planet are omitted from the schedule. Reference 1 indicates that, even with an entirely on-board system, observations of Mars at this time are ineffective in estimating the miss compared to observations of the Earth, despite the large distance to the Earth.

Since the reference trajectory is type II, there is a guidance singularity¹ which, in this case, occurs at 43 days. The first correction cannot be made near this time. For the present reference trajectory there is no performance advantage in making the first correction as early as possible after departing Mars. Thus, the first correction occurs at 84 days, providing the estimation system with a very long time to determine the miss. It should be noted that a somewhat different reference orbit may require an early first correction and, hence, an early determination of the miss. A case of this type occurs in the return leg of the Venus swing-by mission discussed below.

Venus swing-by mission, Earth-Mars leg.- The reference trajectory is type I with a flight time of 170 days. Table III(c) lists the navigation schedule used to generate the data for this leg, and figure 4(a) shows the resulting miss uncertainty. The results are generally similar to those for the outbound leg of the high-speed mission and will not be considered further.

Venus swing-by mission, Mars-Venus leg.- The type I reference trajectory for this leg has a flight time of 185 days and remains at distances of the order of 10^8 km from the Earth throughout the flight. The observation schedule (table III(d)) consists of some observations of Mars early in the flight, radar observations at 1/2-day or 1-day intervals up to the time of the first correction and at 10-day intervals thereafter, and frequent observations of Venus during the final 20 days. Figure 4(b) shows the resulting time history of the rms miss-estimation error.

¹The guidance singularity occurs because $A_2(t_F, t)$ becomes singular when the heliocentric angle to the target position is 180° . In this case, the out-of-plane component of the miss is uncontrollable by velocity corrections and is poorly controllable in the region near the singularity. This does not preclude the possibility of correcting only the controllable components, but such sophistication of the guidance system is not within the scope of this study.

Radar measurements are very effective up to the approach to Venus, and are capable of reducing the miss-estimate error to several hundred kilometers. However, prior to the first correction (at 30 days), the most effective schedule combined both Mars and radar observations. Figure 4(b) compares the results for this region of the mission for three schedules: only on-board observational data, only radar data, and both radar and Mars observations. The schedules with radar data give a much better estimate of the miss than does the schedule with only on-board observations and the combined schedule does somewhat better than the radar-only schedule. This occurs because the radar is unable to estimate the crossrange miss during the early part of this leg. Figure 6 compares the early time history of the error in estimating the crossrange miss for both the combined and radar-only schedules, and shows the importance of the Mars observations for an early determination of this component. However, in the present simulation, this component is only a small fraction of the initial miss (cf. table II), and the radar alone is able eventually to make a good estimate of the crossrange miss. Thus, the principal effect of the early Mars observations is a small saving in the total velocity correction (about 1 m/sec). Of course, if the initial crossrange miss were larger, the Mars observations would give a correspondingly more significant fuel saving.

Venus swing-by mission, Venus-Earth leg.- The type II reference trajectory for this leg has a guidance singularity at 28 days, and a total flight time of 125 days. The distributions of initial deviations and the uncertainty in estimating these deviations are obtained from simulation of the preceding Mars-Venus leg of the mission and are given in table II.

The observation schedule (table III(e), fig. 4(c)) consists of frequent observations of Venus while in the immediate vicinity of that planet and radar observations throughout the flight.

The fuel requirements for this leg are decreased if the first correction is made prior to the guidance singularity, within the first 10 days. The most effective schedule for an early determination of the miss combines information from both the radar and observations of Venus. Figure 4(c) compares the time histories of miss uncertainty during the first 10 days of this leg for three schedules using, respectively, only observations of Venus, only radar data, and both radar data and observations of Venus. It is seen that the combined schedule does better than either of the schedules with only one type of observation. Of course, on the return leg the miss can be estimated very accurately with the radar alone and there would be no reduction in terminal miss performance if the Venus observations were deleted. The principal effect of the Venus observations in the combined schedule is then a modest reduction in velocity-correction requirements (about 3 m/sec in the present example).

Comparison With Performance Predicted by the Optimum Correction-Schedule Theory

The optimum correction schedule and corresponding minimum fuel requirements are computed, as described in appendix A, after an empirical

determination of the optimum timing of the first correction. The timing of the final correction is determined by a specified rms allowable terminal miss which, in the present case, is 2 km.

Performance data from simulation and from the theory are compared in tables IV and V for all legs of both reference missions. Data for three-, four-, and five-correction schedules for both legs of the high-speed mission are contained in table IV and data for four-correction schedules for all legs of the Venus swing-by mission in table V. The specified terminal miss performance is generally not achieved, principally because the miss has not been determined with sufficient accuracy at the time of the final correction. However, performance is generally good because the largest component of the miss is oriented in the downrange direction. This affects only the arrival time as discussed later.

In general, the predicted fuel requirements are optimistic. This is because the theoretical model neglects the uncertainty in the miss estimate at the time of each correction and the miss generated by correction errors other than the cutoff error. Both of these approximations cause the size of the third and subsequent corrections to be underestimated by the theory. The total velocity correction shows good agreement for the four- and five-correction schedules, being within 4 m/sec in every case. Table IV also illustrates the decrease in velocity-correction requirements and the size of each correction with an increase in the number of corrections.

Thus, because of the accuracy achieved with radar observations, the theory of Lawden (ref. 2) gives an adequate first approximation to the optimum correction schedule, velocity-correction requirements, correction size, and their dependence on the number of corrections.

Comparison With Performance of the On-Board Navigation System

The rms total velocity-correction requirements and terminal miss for the system of this report and a system using only on-board observations are compared in table VI. Data for the on-board system are taken from reference 1 and correspond to schedules using four midcourse corrections on each leg with variable time-of-arrival (VTA) guidance corrections where indicated. Data for the present system correspond to the navigation schedules of table III and use fixed arrival-time guidance for all corrections.

The results show a varying amount of fuel saving with the inclusion of ground-based radar data; for the return leg of the high-speed mission there is almost no reduction, but for the outbound leg of the Venus swing-by mission the velocity-correction requirements are cut in half.

Table VI shows a large reduction in downrange miss with the use of radar. Navigation data from on-board observations generally give limited information on the downrange miss until late in the mission, where the fuel required to correct this miss is large. This deficiency of the on-board system made it advisable to utilize VTA guidance for the final one or two corrections in reference 1 in order to reduce the fuel requirements substantially. This type of guidance corrects only the lateral miss and ignores the downrange miss

remaining from earlier fixed time-of-arrival corrections; hence it produces the large downrange miss seen in table VI for the on-board system. On the other hand, the system of this study improves the estimate of all components of the miss everywhere in the flight; consequently, only minor fuel saving would occur if VTA corrections were made during the approach phases.

The principal effect of the downrange miss is a change in the time of pericenter. This is seen from the following linearized equations for the errors in pericenter position and time (see ref. 5):

$$\delta \bar{r}_p = (\bar{u}\bar{u}^T + \bar{n}\bar{n}^T) \delta \bar{r}(t_f) - \frac{R_p}{V_p} \bar{p}\bar{u}^T \delta \bar{v}(t_f)$$

$$\delta t_p = -\frac{1}{V_p} \bar{p}^T \delta \bar{r}(t_f) - \frac{R_p}{V_p^2} \bar{u}^T \delta \bar{v}(t_f)$$

where \bar{u} , \bar{p} , and \bar{n} form an orthonormal vector triad with \bar{u} along the reference pericenter position (radial) and \bar{p} along the reference pericenter velocity (downrange). To first order, the downrange miss, $\bar{p}^T \delta \bar{r}(t_f)$, affects only the time of pericenter. The reduction in downrange miss shown in table VI corresponds to a reduction in the rms pericenter time error from several minutes for the on-board system to several seconds. However, the timing error associated with the on-board system requires only modest adjustments in entry range for landing at a fixed site on Earth.

Of particular interest in manned missions is the control of pericenter radius to lie within a safe entry corridor both at Mars and at the critical return to Earth. It can be seen from the above equation that the error in pericenter radius, $\bar{u}^T \delta \bar{r}_p$, is simply the radial miss, which, in table VI, is generally cut in half when radar data are included.

CONCLUDING REMARKS

This paper examines the performance of midcourse guidance and navigation systems for manned interplanetary missions when both radar and on-board observational data are available.

The investigation of appropriate observation schedules for such systems shows that radar generally provides superior data and will be sufficient for best performance during most of the mission. However, during the approach to distant planets on-board observations are essential to improve the miss estimate to the accuracy required for entry or for close approach of manned vehicles. In addition, on-board observations during departure from distant planets will usually reduce fuel requirements.

It may be noted that the amount of radar data assumed in this study is quite small compared to what would be available in the real case. More intensive use of radar data would improve performance somewhat over that shown in

this report, but the improvement would be limited because the trajectory is already estimated with the minimal data nearly as accurately as it can be controlled.

When the trajectory is estimated more accurately than it can be controlled, as in the present study, the optimum correction schedule is independent of the observation schedule. This feature, together with several simplifying assumptions, allows application of the work of Lawden (ref. 2) to the a priori computation of an optimum correction schedule. The minimum velocity correction requirements, correction size, and the dependence of these parameters on the number of corrections are readily determined by the theory. An optimum number of corrections, on the order of 8 to 10 for the cases studied here, is given by the theory. However, this can be reduced to 4 or 5 corrections without significant fuel penalty. Results from simulation of the system gave fair agreement with the theory.

The combined radar and on-board data are shown to give fair improvement in both fuel requirements and miss performance over a purely on-board system. However, it should be noted that the on-board system for which the comparison was made used a minimal amount of data and sufficient additional data could be expected to improve its performance.

The performance obtained from simulation of the guidance and navigation system of this study gave velocity-correction requirements ranging from 18 to 24 m/sec on the various legs of the two missions. The rms miss in pericenter radius was less than 2.8 km at Earth and Mars and 6 km at Venus. The rms downrange miss varied from 2 to 22 km.

Ames Research Center
National Aeronautics and Space Administration
Moffett Field, Calif., June 13, 1966
125-17-05-08

APPENDIX A

DERIVATION OF OPTIMUM VELOCITY-CORRECTION SCHEDULE

The correction schedule is designed to null the miss. The optimum schedule is one which accomplishes this end at least cost, that is, for the least amount of corrective fuel. In general, the fuel requirements vary with the observation schedule as well as the correction schedule, and the general problem is of such complexity that no analytical solution has thus far been given. However, because of the inclusion of radar data in this study, the miss is generally estimated better than it can be controlled. Consequently, certain simplifications can be made. First, the optimum correction schedule will, for the most part, be independent of the observation schedule. Secondly, the first midcourse correction will null almost all the miss generated by injection errors, and subsequent midcourse corrections will correct principally for miss generated by random errors in the preceding correction. Of course, if the estimation and correction systems are so accurate that the miss following the first correction is acceptable, then the scheduling problem will be trivial. But for the assumed state of the art, the miss generated by errors in each correction is significant. This miss has a lower bound determined by the thrust cutoff error and is approximately proportional to the time to go.

In the following, the general equations for the statistical properties of the velocity corrections are derived and a statement of the optimum scheduling problem is given. Next, a list of simplifying assumptions is discussed and, with these assumptions, an optimum correction schedule is derived. The simplified problem has been solved by Lawden (ref. 2), and the principal features of that solution and its application to the present simulations will be discussed.

General Problem

Velocity corrections.- The guidance correction is an attempt to null the miss. For fixed time-of-arrival (FTA) guidance, the miss is the position deviation from the reference position at the reference time of arrival, t_F . If the quantities of interest are assumed to be adequately represented by the linearized equations of motion, the miss is related linearly to the current state deviation:

$$m(t) = B(t_F, t)x(t) \quad (A1)$$

where, for FTA guidance, B is the 3×6 matrix taken from the upper half of the transition matrix (ref. 1):

$$B(t_F, t) = [A_1(t_F, t) \quad A_2(t_F, t)] \quad (A2)$$

More generally, for arbitrary linear guidance laws, the miss can be expressed as in equation (A1), but with different expressions for B (ref. 5).

The current state, x , can be given in terms of its estimated value, \hat{x} , and the error in the estimation, \tilde{x} , as

$$\text{Similarly, } \left. \begin{aligned} x(t) &= \hat{x}(t) + \tilde{x}(t) \\ m(t) &= \hat{m}(t) + \tilde{m}(t) \end{aligned} \right\} \quad (\text{A3})$$

where

$$\left. \begin{aligned} \hat{m}(t) &= B(t_F, t)\hat{x}(t) \\ \tilde{m}(t) &= B(t_F, t)\tilde{x}(t) \end{aligned} \right\} \quad (\text{A4})$$

The commanded velocity correction is computed from the estimated miss. (A justification for this procedure is given in reference 6.) For FTA guidance, the correction is

$$\Delta V_c = -A_2^{-1}(t_F, t)\hat{m}(t^-) \quad (\text{A5})$$

where the symbol t^- refers to time just prior to t . This velocity correction is carried out with random error, η , so that the actual correction is

$$\Delta V = \Delta V_c + \eta \quad (\text{A6})$$

The miss vector.- The actual miss is a step function with changes at each correction. Its initial value is specified by the injection errors, x_0 ; hence, prior to the first correction, the miss is

$$m(t) = B(t_F, t_0)x_0, \quad t_0 < t < t_j \quad (\text{A7})$$

After each correction, the miss is given by the miss prior to the correction and the change due to the correction. In the interval (t_j, t_{j+1}) between the j th and $(j+1)$ st correction, the miss is:

$$m(t) = m(t_j^-) + A_2(t_F, t_j)\Delta V_j$$

From equations (A3) and (A6), this becomes

$$m(t) = \tilde{m}(t_j^-) + A_2(t_F, t_j)\eta_j, \quad t_j < t < t_{j+1} \quad (\text{A8})$$

That is, the miss following a correction is due to the miss uncertainty prior to the correction and the error in making the correction.

Statistical properties.- The navigation and guidance process is subject to random errors, so that the parameters which give the performance of the system - the final-miss and total-fuel - are random variables that must be dealt with statistically. All input random variables - injection, measurement, and correction errors - are assumed to be gaussian distributed with zero means. Since the equations of motion have been linearized, the random vectors of interest are linear combinations of the input random variables and are, therefore, gaussian distributed with zero means. In that case, their statistical properties are specified by their covariance matrices.

Assuming the state estimate has been made using the Kalman filter, then \tilde{x} and \hat{x} are uncorrelated and, consequently, \tilde{m} and \hat{m} are also uncorrelated. The covariances M , \hat{M} , and \tilde{M} are defined by:

$$M = E[mm^T], \text{ etc.}$$

where E is the expectation operator. These are positive definite matrices related by

$$M = \hat{M} + \tilde{M} \quad (A9)$$

From equations (A7) and (A8), one can obtain

$$\left. \begin{aligned} M(t) &= B(t_F, t) \text{PAR}_0 B^T(t_F, t) \equiv M_0, & t_0 < t < t_1 \\ M(t) &= \tilde{M}(t_j^-) + A_2(t_F, t) S_j A_2^T(t_F, t), & t_j < t < t_{j+1} \end{aligned} \right\} \quad (A10)$$

where PAR_0 and S_j are the covariance matrices, respectively, of the injection errors and the errors in making the j th correction. The second of these equations uses the independence between correction errors, η_j , and estimation errors, $\tilde{m}(t_j^-)$.

Define the covariance matrix, C_j , as $E[\Delta V_C \Delta V_C^T]$. This can be written, from equations (A5) and (A9), as

$$C_j = A_2^{-1}(t_F, t_j) [M(t_j^-) - \tilde{M}(t_j^-)] A_2^{-1T}(t_F, t_j) \quad (A11)$$

The actual correction (eq. (A6)) then has the covariance

$$V_j = C_j + S_j \quad (A12)$$

where statistical independence between the commanded correction and the correction error has been assumed.

Problem of the optimum correction schedule.- If N midcourse velocity corrections are made between injection, t_0 , and arrival, t_F , their execution times, $\{t_1, \dots, t_N\}$, are called the correction schedule. The optimum scheduling problem to be discussed is stated as follows:

Given that N corrections are made in (t_0, t_F) , find the sequence of execution times

$$t_0 < t_1 < \dots < t_N < t_F$$

such that the sum of the rms velocity corrections,

$$T = \sum_{j=1}^N \sqrt{\text{trace}(V_j)}$$

is a minimum, and the rms miss following the last correction is

$$\sqrt{\text{trace}[M(t_N^+)]} = m_a$$

Here, m_a is some acceptable numerical value of the rms final miss.

The parameter m_a represents the desired terminal miss performance and affects velocity-correction requirements. A lower value of m_a (i.e., better terminal miss performance) increases the required total correction; that is, the choice of m_a involves a trade-off between fuel and terminal miss. It should also be recognized that, regardless of the choice of m_a , the terminal-miss performance can be limited by other factors inherent in the navigation system.

The choice of cost function T , as given above, is motivated by the need for mathematical tractability. A more appropriate criterion would be the minimization of expected fuel requirements which, for a vehicle of constant mass, is given by the sum of the expected velocity-correction magnitudes rather than the sum of rms values:

$$T' = \sum_{j=1}^N E \{ |\Delta V_j| \}$$

However, if the magnitudes of the several corrections are similarly distributed (i.e., the distribution curves have the same shape and differ only in scale), then the rms and mean magnitudes of each correction are always in the same ratio. Previous experience shows that such proportionality is a fair approximation in actual practice. Thus, minimizing the sum of rms correction magnitudes is sufficiently close to minimizing the fuel requirements to justify the choice of the former as the optimality criterion.

Simplifying Assumptions

Independence of correction and observation schedules. - For convenience, equations (A10), (A11), and (A12) are repeated:

For $j = 1, 2, \dots, N$

$$V_j = A_2^{-1}(t_F, t_j) [M(t_j) - \tilde{M}(t_j)] A_2^{-1T}(t_F, t_j) + S_j$$

$$M(t) = \begin{cases} M_0 & t_0 < t < t_1 \\ \tilde{M}(t_j) + A_2(t_F, t_j) S_j A_2^T(t_F, t_j) & t_j < t < t_{j+1} \end{cases}$$

In general, the total fuel depends on the performance of the estimation system through the terms $\tilde{M}(t_j)$, $j = 1, 2, \dots, N$. The analytical problem presented by the general case is unsolved, but adequate schedules can be obtained empirically (e.g., ref. 4).

On the other hand, if the term $\tilde{M}(t_j^-)$ can be neglected, then the correction schedule is independent of the observation schedule for the interval (t_{j-1}, t_j) . Further, if all the terms $\tilde{M}(t_j^-)$ $j = 1, \dots, N$ can be neglected, the correction schedule is entirely independent of the observation schedule.

It is clear that if the miss were perfectly estimated at the time of the j th correction then $\tilde{M}(t_j^-)$ would be zero. In general, $\tilde{M}(t_j^-)$ is not zero and it is of interest to state how well the miss must be estimated in order to neglect $\tilde{M}(t_j^-)$.

Assumption 1.

$\tilde{M}(t_j^-)$ can be neglected if

$$(a) \text{tr} [\tilde{M}(t_j^-)] \ll \text{tr} [M(t_j^-)]$$

$$(b) \text{tr} [\tilde{M}(t_j^-)] \ll \text{tr} [A_2(t_F, t_j) S_j A_2^T(t_F, t_j)]$$

The first condition states that the miss uncertainty is small compared to the miss, from which

$$V_j = A_2^{-1}(t_F, t_j) M(t_j^-) [A_2^{-1}(t_F, t_j)]^T + S_j \quad (A13)$$

The second condition states that the miss has been estimated better than it can be corrected, that is, the miss following the j th correction is due almost entirely to errors in making the correction.

$$M(t) = \begin{cases} M_0 & t_0 < t < t_1 \\ A_2(t_F, t_j) S_j A_2^T(t_F, t_j) & t_j < t < t_{j+1} \end{cases} \quad (A14)$$

Simplified correction-error model. - The covariance matrix, S_j , is an important parameter when the correction and observation schedules are independent. The error model, already discussed in the text, is taken from reference 1, appendix A.

$$S_j = \left[\begin{array}{c} \overline{\kappa^2} + \frac{\overline{\epsilon^2}}{\overline{c_j^2}} \\ \overline{c_j^2} \end{array} \right] C_j + \frac{1}{2} \overline{\gamma^2} \left[\overline{c_j^2} I - C_j \right]$$

where $\overline{\kappa^2}$, $\overline{\gamma^2}$, and $\overline{\epsilon^2}$ are the variances, respectively, of the proportional, aiming, and cutoff errors, and $\overline{c_j^2}$ is the mean-square correction, $\text{tr}(C_j)$.

If the commanded correction is almost spherically distributed so that $C_j \cong \frac{1}{3} \overline{c_j^2} I$, then S can be approximated by

$$S_j \cong \left[(\overline{\kappa^2} + \overline{\gamma^2}) \overline{c_j^2} + \overline{\epsilon^2} \right] \frac{1}{3} I$$

For the present Mars mission studies, the rms errors are assumed to be

$$\sqrt{\kappa^2} = 0.01, \quad \sqrt{\gamma^2} = 1^\circ, \quad \sqrt{\epsilon^2} = 0.2 \text{ m/sec}$$

In this case, the cutoff error is the dominant error, statistically, when $\sqrt{c_j^2}$ is about 5 m/sec or less. The first correction is usually large, statistically, but the remaining corrections are usually small, allowing the following approximation:

Assumption 2.

For each correction except the first, the commanded velocity correction is distributed almost spherically and the cutoff error is, statistically, the dominant error in making the correction:

$$S_j \approx \frac{\overline{\epsilon^2}}{3} I \quad j = 2, \dots, N \quad (\text{A15})$$

Approximation of V_j . The actual correction consists of the commanded velocity correction and the errors in executing the correction (eq. (A12)). The error term is usually small by comparison, so that one can assume:

Assumption 3.

The errors in making a correction are small compared to the actual correction

$$\text{tr}(S_j) \ll \overline{c_j^2}$$

In this case, equation (A12) becomes

$$V_j = C_j \quad (\text{A16})$$

The first correction is usually large and assumption 3 readily applies. For the remaining corrections, in view of assumption 2, assumption 3 is satisfied if $\overline{\epsilon^2} \ll \overline{c_j^2}$. For the assumed value $\sqrt{\overline{\epsilon^2}} = 0.2$ m/sec, assumption 3 is valid when the rms correction, $\sqrt{\overline{c_j^2}}$, is 1 m/sec or greater. This should normally be the case, since the operation of thrust devices near the level of the errors in thrusting is generally avoided.

Approximation of $A_2(t_F, t)$. The columns of this matrix are the derivatives of position at t_F with respect to the components of velocity at t , evaluated on the reference orbit.

If the gravitational acceleration on the deviated path is identical to the gravitational acceleration on the reference path at every time, then the deviation equations of motion are those of a straight line; therefore

$$A_2(t_F, t) = (t_F - t)I \quad (\text{A17})$$

For the heliocentric orbits occurring in interplanetary missions, the difference in gravitational acceleration on nearby orbits is very small so that equation (A17) remains a fair approximation over extended periods of time.

The maximum interval for which this approximation remains valid is not precisely known, but an absolute upper limit is given by the fact that $A_2(t_F, t)$ becomes singular in Keplerian motion when the interval $t_F - t$ corresponds to a difference of 180° in true anomaly.

Equation (A17) is used in the remainder of this analysis in the equations governing the second and later corrections, which normally occur when much less than half an orbit remains to be traversed to the target position. However, equation (A17) is often a poor approximation at the time of the first correction. The matter of approximations to the transition matrix is discussed at length in reference 7.

Simplified Problem and Its Solution

Optimum correction schedule for the simplified problem. - In the simplified problem only assumption 3 is applied for the first correction. All three assumptions and the approximation given in equation (A17) are used for the remaining corrections.

If $c_1(t_1)$, $m_1(t_1)$ are the rms first correction and miss following the first correction, then

$$\begin{aligned}\sqrt{\text{tr}(V_1)} &= c_1(t_1) \\ \sqrt{\text{tr}(V_2)} &= m_1(t_1)/(t_F - t_2) \\ \sqrt{\text{tr}(V_j)} &= \sqrt{\epsilon^2}(t_F - t_{j-1})/(t_F - t_j) \quad j = 3, \dots, N\end{aligned}$$

The dimensionless time to go is defined as

$$\tau_j = (t_F - t_j)/(t_F - t_0).$$

The sum of the rms corrections is then:

$$T = c_1(t_1) + \frac{m_1(t_1)}{t_F - t_0} \frac{1}{\tau_2} + \sqrt{\epsilon^2} \sum_{j=3}^N \frac{\tau_{j-1}}{\tau_j} \quad (\text{A18})$$

From equations (A14), (A15), and (A17) the rms final miss is entirely determined by the cutoff error in the last midcourse correction,

$$m(t_N^+) = (t_F - t_N) \sqrt{\epsilon^2}$$

Since the rms final miss is specified to be equal to m_a , then the timing of the final correction is specified by

$$\tau_N = \frac{m_a}{\sqrt{\epsilon^2}(t_F - t_0)} \quad (\text{A19})$$

It should be noted that the simplified equation for the final miss accounts only for the miss generated by the cutoff error in the final correction and therefore underestimates the true value of the final miss to the extent that the miss estimate uncertainty at t_N contributes to the terminal miss.

The independent parameters of the correction schedule are now t_1 , $\tau_2, \dots, \tau_{N-1}$ and T has an extreme (minimum) at

$$\begin{aligned} \frac{\partial T}{\partial t_1} &= 0 \\ \frac{\partial T}{\partial \tau_j} &= 0 \quad j = 2, \dots, N-1 \end{aligned}$$

From equation (A18)

$$\left. \begin{aligned} \frac{\partial T}{\partial t_1} &= \frac{\partial c_1}{\partial t_1} + \frac{1}{t_F - t_2} \frac{\partial m_1}{\partial t_1} = 0 \\ \frac{\partial T}{\partial \tau_2} &= - \frac{m_1}{t_F - t_0} \frac{1}{\tau_2^2} + \sqrt{\epsilon^2} \frac{1}{\tau_3} = 0 \\ \frac{\partial T}{\partial \tau_j} &= \sqrt{\epsilon^2} \left(- \frac{\tau_{j-1}}{\tau_j^2} + \frac{1}{\tau_{j+1}} \right) = 0 \quad j = 3, \dots, N-1 \end{aligned} \right\} \quad (A20)$$

Except for the first, these equations are readily solved (algebra omitted), giving

$$\tau_j = \left(\frac{m_a}{m_1} \right)^{\frac{j-1}{N-1}} \frac{m_1}{\sqrt{\epsilon^2}(t_F - t_0)} \quad j = 2, \dots, N \quad (A21)$$

That is, the optimum schedule for t_2, \dots, t_N depends on the timing of the first correction only through the rms miss, m_1 , inherited from the first correction. The sum of the rms velocity corrections is now

$$T = c_1 + \sqrt{\epsilon^2}(N-1) \left(\frac{m_1}{m_a} \right)^{\frac{1}{N-1}} \quad (A22)$$

where T is given as a function of t_1 only. If t_1 can be determined (empirically) such that T is a minimum, then all of equations (A20) are satisfied and the entire schedule $\{t_1, \dots, t_N\}$ is the solution of the optimum scheduling problem.

Several consequences of equation (A21) should be noted. The timing of the j th correction is a fixed fraction of the timing of the preceding correction:

$$\frac{\tau_j}{\tau_{j-1}} = \left(\frac{m_a}{m_1} \right)^{\frac{1}{N-1}} \quad j = 2, \dots, N \quad (A23)$$

For all corrections after the first, the rms miss is reduced by a fixed fraction:

$$\frac{m(t_j^+)}{m(t_j^-)} = \left(\frac{m_a}{m_1}\right)^{\frac{1}{N-1}} \quad j = 2, \dots, N \quad (A24)$$

and the rms correction is constant:

$$c_j = \sqrt{\epsilon^2} \left(\frac{m_1}{m_a}\right)^{\frac{1}{N-1}} \quad j = 2, \dots, N \quad (A25)$$

Equation (A18) and its solution are given in reference 2. The optimum schedule represents a compromise between two opposing effects. If the j th correction is delayed, the miss generated by random errors in the j th correction will be less and subsequent corrections will require less fuel. On the other hand, a delay increases the fuel required for the j th correction.

Computation of t_1 .- The timing of the first corrections is left to empirical determination. Hence, only assumption 3 need apply at t_1 .

It is not difficult to determine t_1 empirically if one assumes a reasonable observation schedule for the initial part of the flight and then uses a computer program which simulates the statistical performance of the guidance and navigation system, obtaining $m_1(t^+)$ and $c_1(t)$. These parameters are, respectively, the rms postcorrection miss and velocity correction if a correction is made at t . Equation (A22) can be used to compute the total velocity-correction requirements as a function of the time of the first correction, from which the optimum time, t_1 , is selected.

Number of corrections.- An optimum value of N , found by minimizing T (eq. (22)) with respect to N , is reported in reference 2. The optimum N is one of the neighboring integers of

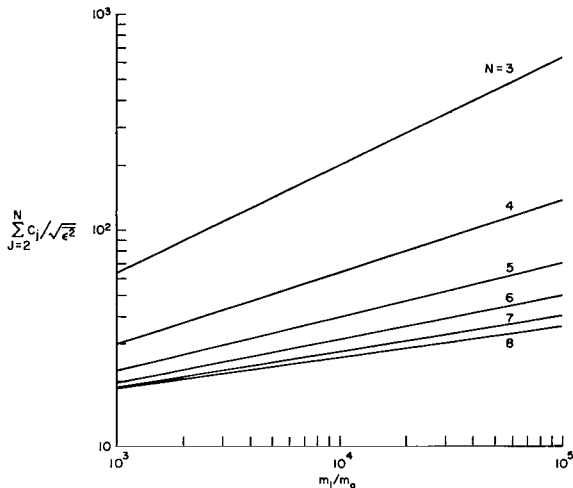
$$N^* = 1 + \ln\left(\frac{m_1}{m_a}\right)$$

For typical values of the ratio m_1/m_a found in this study, 10^3 to 10^4 , we have

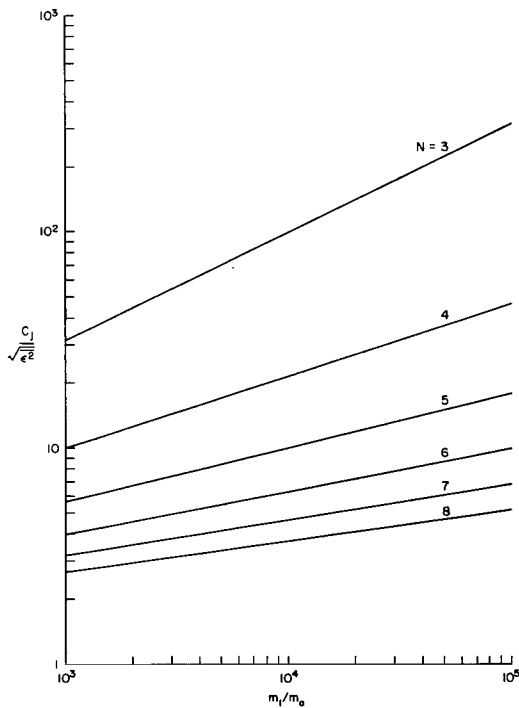
$$N^* = 8.1 \text{ to } 10.2$$

However, practical difficulties, which will be discussed below, arise with such a large number of corrections, and the fuel saved by using 8 or 10 corrections rather than, say, 4 or 5 may not be significant.

Data illustrating the dependence of fuel requirements and correction magnitudes on the number of corrections are given in sketches (a) and (b). The first correction, which accounts principally for injection errors, is very nearly independent of the number of corrections, but fuel requirements for the remaining corrections depend on N (see eq. (A22)). Sketch (a) gives the sum



Sketch (a)



Sketch (b)

of the rms velocity corrections for all corrections except the first versus the parameter m_1/m_0 for various values of N . It is seen that the fuel required decreases with increases in the number of corrections, but for large N the advantage of further increases in N diminishes.

Sketch (b) shows that the size of individual corrections also decreases with increasing N and soon approaches the size of the cutoff error. Note also that for the low values of N the individual corrections can be large enough that significant miss may be generated by correction errors other than the cutoff error. In this case, poorer agreement with the theoretical fuel requirements is expected.

A final point of interest is that the time interval between the last few corrections becomes small as N increases. This can be seen from equation (A23).

In the simulations of this study, $N = 4$ was selected as a compromise between total fuel and correction size.

Off-optimum timing. - It is of interest to determine how critical the timing is of each correction.

Usually, the fuel requirement per unit miss rises very slowly with time in the region of the first correction (although this is not always the case). In the present simulation, the miss is determined at the time of the first correction to the order of the miss generated by errors in the first correction or better. In this case, there is very little penalty associated with delays in the first correction. In some cases, a guidance singularity occurs soon after injection so that delays beyond the optimum timing of the first correction may cause more significant penalties.

On the other hand, if the first correction is made earlier than the optimum time, the principal penalty arises from a poorer estimation of the miss. For instance, if the correction is made early enough that the post-correction miss is twice the value for the optimum timing, the fuel for the remaining corrections will be increased by a factor of $2^{1/(N-1)}$, while the fuel for the first corrections will remain very nearly the same; that is,

$$T(2m_1) = T(m_1) + [2^{1/(N-1)} - 1][T(m_1) - c_1]$$

where m_1 refers to the miss following the optimally timed first correction.

For corrections 2, . . . , N-1 (t_N remains fixed to satisfy the miss performance criterion), let the timing of the j th correction be changed from the optimum time, t_j^* , by the amount Δt_j . This yields the change in the sum of rms velocity corrections (algebra omitted)

$$\frac{\Delta T}{\sqrt{\epsilon^2(m_1/m_a)} \frac{1}{N-1}} = \frac{[\Delta t_j / (t_F - t_j^*)]^2}{1 - \Delta t_j / (t_F - t_j^*)}$$

In this equation the penalty, ΔT , has been made dimensionless by a factor recognized as the rms size of the individual corrections. The penalty is greater for a delay (positive Δt_j) than for correcting early by the same amount, and, of course, it becomes arbitrarily large as Δt_j approaches $t_F - t_j^*$. A penalty of 1 percent of the individual correction is obtained for an off-optimum timing of

$$\frac{\Delta t_j}{t_F - t_j^*} = \pm 0.1$$

Similarly, a 10-percent penalty is incurred for timing errors of

$$\frac{\Delta t_j}{t_F - t_j^*} = +0.27, -0.37$$

This is considered a small penalty for fairly large percentage changes in timing and the correction schedule appears to have a broad optimum.

REFERENCES

1. White, John S.; Callas, George P.; and Cicolani, Luigi S.: Application of Statistical Filter Theory to the Interplanetary Navigation and Guidance Problem. NASA TN D-2697, 1965.
2. Lawden, Derek F.: Optimal Programme for Correctional Manoeuvres. Astro-Nautica Acta, vol.6, 1960, pp. 195-205.
3. Smith, Gerald L.; and Harper, Eleanor V.: Midcourse Guidance Using Radar Tracking and On-Board Observation Data. NASA TN D-2238, 1964.
4. Denham, Walter F.; and Speyer, Jason L.: Optimal Measurement and Velocity Correction Programs for Midcourse Guidance. AIAA paper 63-222, 1963.
5. Cicolani, Luigi S.: Linear Theory of Impulsive Velocity Corrections for Space Mission Guidance. NASA TN D-3365, 1966.
6. Potter, James E.: A Guidance-Navigation Separation Theorem. AIAA paper 64-653, 1964.
7. White, John S.: Simplified Calculation of Transition Matrices for Optimal Navigation. NASA TN D-3446, 1966.

TABLE I.- REFERENCE TRAJECTORY PARAMETERS

Trajectory and leg	Departure conditions				Arrival conditions		
	Date	Velocity, km/sec	Altitude, km	Trip time, days	Date	Velocity, km/sec	Altitude, km
High speed Earth to Mars	May 31.57, 1971	11.761	160.00	112.43	Sept. 21.00, 1971	8.49	-3.54
High speed Mars to Earth	Sept. 27.22, 1971	9.813	300.32	190.77	April 4.98, 1972	14.26	-2.96
Venus swing-by Earth to Mars	Sept. 9.49, 1975	12.020	159.27	170.01	Feb. 26.49, 1976	7.76	26.43
Venus swing-by Mars to Venus	March 27.55, 1976	7.097	499.90	185.54	Sept. 29.10, 1976	14.69	3363.59
Venus swing-by Venus to Earth	Sept. 28.54, 1976	14.992	3349.96	124.94	Jan. 31.48, 1977	13.91	-11.06

Velocity and altitude are at periapse of the vacuum hyperbola. Dates are given in universal time.

TABLE II.- RMS INJECTION, CORRECTION, AND MEASUREMENT ERRORS¹

Injection errors (Mars and Earth injection)²

Altitude	3.2187 km (2 miles)	4.47 m/sec (10 mph)
Downrange	4.8285 km (3 miles)	1.788 m/sec (4 mph)
Crossrange	1.60935 km (1 mile)	1.341 m/sec (3 mph)

Corresponding initial miss, km

Mission	Leg	Altitude	Downrange	Crossrange	Total
High speed	Outbound	62,000	170,000	27,600	183,000
	Return	104,000	114,000	9,200	155,000
Venus swing-by	Outbound	193,000	198,000	79,400	288,000
	Mars-Venus	122,000	107,000	5,940	163,000

Initial miss³- return leg, Venus swing-by mission, km

	Altitude	Downrange	Crossrange	Total
Miss	187,000	172,000	8,260	255,000
Miss uncertainty	164,000	146,000	2,840	219,000

Errors in making velocity corrections

Magnitude, $\sqrt{\kappa^2}$	1 percent
Direction, $\sqrt{\gamma^2}$	1°
Cutoff, $\sqrt{\epsilon^2}$	0.2 m/sec

Errors in measuring velocity corrections

1 cm/sec rms equally likely in all directions

Theodolite observation errors

Instrument error, $\sqrt{q^2}_{inst}$	10 seconds of arc
Radius uncertainty/planet radius, $\sqrt{b^2}$	0.001
Position uncertainty, $\sqrt{\delta R_S^2}$	1 km

¹All errors are assumed gaussian distributed with zero means.

²The initial uncertainty is identical to the injection errors except on the return leg of the Venus swing-by mission.

³These values are obtained from simulation of the preceding Mars-Venus leg, using the navigation schedule of table III(d).

TABLE III.- NAVIGATION SCHEDULE¹

(a) High-speed mission, outbound leg

Initial time, days	Observation interval, days	Group interval, days	Observation		Type (2)
			Number	Group	
0.1	0.2		5		R
1.10		Velocity correction			
1.50	.5	2.0	15	5	R,2E
93.50		Velocity correction			
94.00	.1	1.0	75	15	2R,3M
109.0	.1		2		R
109.3	.123		14		M
110.95		Velocity correction			
111.00	.048		28		M
112.32		Velocity correction			
112.432		Pericenter (Mars)			

Total observations - 42 radar, 10 Earth, 87 Mars

¹The table is read as follows: line 3, for example, specifies that each group of observations consists of one radar and two theodolite observations separated by 0.5-day intervals. This group is repeated 10 times, beginning every second day.

²R - radar; E, M, V - theodolite observations of Earth, Mars, or Venus.

TABLE III.- NAVIGATION SCHEDULE¹- Continued

(b) High-speed mission, return leg

Initial time, days	Observation interval, days	Number	Observation	
				Type (2)
3.0	4.0	20		R
84.0		Velocity correction		
101.0	10.0	8		R
172.0		Velocity correction		
174.0	2.0	8		R
189.0	.1	3		R
189.3		Velocity correction		
189.4	.2	6		R
189.5	.05	3		R
190.65		Velocity correction		
190.765		Perigee		
Total - 48 radar observations				

^{1,2}See footnotes page 30.

TABLE III.- NAVIGATION SCHEDULE¹ - Continued

(c) Venus swing-by mission, Earth-Mars leg

Initial time, days	Observation interval, days	Group interval, days	Observation		
			Number	Group	Type (2)
0.1	0.1		8		R
.9		Velocity correction			
1.0	.5		5		R
3.0	1.0		7		R
100.0	10.0		5		R
143.6		Velocity correction			
145.0	1.0	4	16	4	R,3M
165.0	1.0		7		M
168.76		Velocity correction			
168.28	.02		31		M
169.0	.02		44		M
169.90		Velocity correction			
170.008		Pericenter (Mars)			
		Total - 29 radar, 94 Mars			

^{1,2}See footnotes page 30.

TABLE III.- NAVIGATION SCHEDULE¹- Continued

(d) Venus swing-by, Mars-Venus leg

Initial time, days	Observation interval, days	Group interval, days	Observation		
			Number	Group	Type (2)
1.0	0.5		4		R
3.0	.5	2	30	10	2R,M
22.5			1		R
23.0	1	2	4	2	M,R
27.0		Velocity correction			
30.0	1	10	14	7	R,M
100.0	1	10	12	6	R,V
160.0					R
160.1		Velocity correction			
160.5	.1		5		V
161.0	.5		16		V
170.0	.2		1		R
			63		V
			1		R
183.85		Velocity correction			
183.9	.05		30		V
185.4		Velocity correction			
185.45			1		V
185.545		Pericenter (Venus)			

Total - 43 radar, 19 Mars, 121 Venus

^{1,2}See footnotes page 30.

TABLE III.- NAVIGATION SCHEDULE¹- Concluded

(e) Venus swing-by mission

Initial time, days	Observation interval, days	Group interval, days	Observation		
			Number	Group	Type (2)
0.2	0.02		30		V
.62	.03		2		R
.7	.1		13		3V,R,9V
2.0		Velocity correction			
2.5			1		R
3.0	1.0	2.0	10	5	V,R
20.0	10.0		8		R
95.0			1		R
97.75		Velocity correction			
100.5	1.5		15		R
123.0			1		R
123.17		Velocity correction			
123.2	.2		9		R
124.83		Velocity correction			
124.945		Perigee			
Total - 49 Venus, 42 radar					

^{1,2}See footnotes page 30.

TABLE IV.- COMPARISON WITH PREDICTED PERFORMANCE (RMS)

(a) High-speed mission, outbound leg; flight time = 112.432 days								
N = 3			N = 4			N = 5		
t_j	c_j		t_j	c_j		t_j	c_j	
	Theory	Simulation		Theory	Simulation		Theory	Simulation
0.55	10.77	10.77	1.10	11.03	11.03	0.24	10.37	10.37
107.00	9.20	8.93	93.50	2.56	2.42	71.00	1.38	1.19
112.32	9.20	17.00	110.95	2.56	3.60	106.50	1.38	1.46
			112.32	2.56	3.41	111.60	1.38	1.45
						112.32	1.38	1.66
Total ΔV , m/sec	29.17	36.72		18.70	20.48		15.90	16.19
Terminal miss, km	2.0	4.2		2.0	5.4		2.0	3.4
(b) High-speed mission, return leg; flight time = 190.765 days								
84.0	10.15	10.15	84.0	10.15	10.15	84.0	10.15	10.15
185.5	9.10	7.94	172.0	2.55	2.28	155.30	1.35	1.19
190.65	9.10	12.43	189.30	2.55	2.67	185.50	1.35	1.41
			190.65	2.55	5.36	190.00	1.35	1.86
						190.65	1.35	1.64
Total ΔV , m/sec	28.35	30.52		17.80	20.48		15.55	16.30
Terminal miss, km	2.0	4.5		2.0	3.8		2.0	3.1

Note: N = number of corrections
 t_j = time of jth correction
 c_j = rms value of jth correction

TABLE V.- COMPARISON WITH PREDICTED PERFORMANCE - VENUS SWING-BY MISSION

Leg	Outbound			Mars - Venus			Return		
Flight time, days	170.008			185.545			124.945		
N	4			4			4		
	t_j	c_j		t_j	c_j		t_j	c_j	
		Theory	Simulation		Theory	Simulation		Theory	Simulation
	0.90	10.09	10.09	27.0	7.56	7.56	2.0	10.48	10.48
	143.60	3.02	3.32	160.10	2.90	2.85	97.75	3.04	3.71
	168.26	3.02	3.20	183.85	2.90	3.81	123.17	3.04	4.16
	169.89	3.02	4.18	185.40	2.90	4.13	124.83	3.04	5.09
Total ΔV , m/sec		19.15	20.82		16.26	18.37		19.70	23.45
Terminal miss, km		2.0	17.6		2.0	22.1		2.0	3.2

Note: N = number of corrections

t_j = time of j th correction

c_j = rms value of j th correction

TABLE VI. - COMPARISON OF PERFORMANCE WITH ON-BOARD SYSTEM¹

Mission	High speed				Venus swing-by					
Leg	Outbound		Return		Outbound		Mars - Venus		Return	
Navigation data	On-board (2)	On-board and radar	On-board (2)	Radar	On-board (2)	On-board and radar	On-board (3)	On-board and radar	On-board (3)	On-board and radar
Total ΔV	28.86	20.48	20.84	20.84	41.61	20.82	34.30	18.37	29.75	23.45
Radial miss	4.8	2.8	5.0	2.2	4.6	2.1	9.6	5.6	4.2	1.8
Downrange miss	1173	4.0	741	2.2	590	17.4	540	21.3	518	2.1
Total miss		5.3		3.8		17.6		22.1		3.2

¹Four midcourse corrections on each leg

²Last two corrections use variable arrival-time guidance

³Last correction uses variable arrival-time guidance



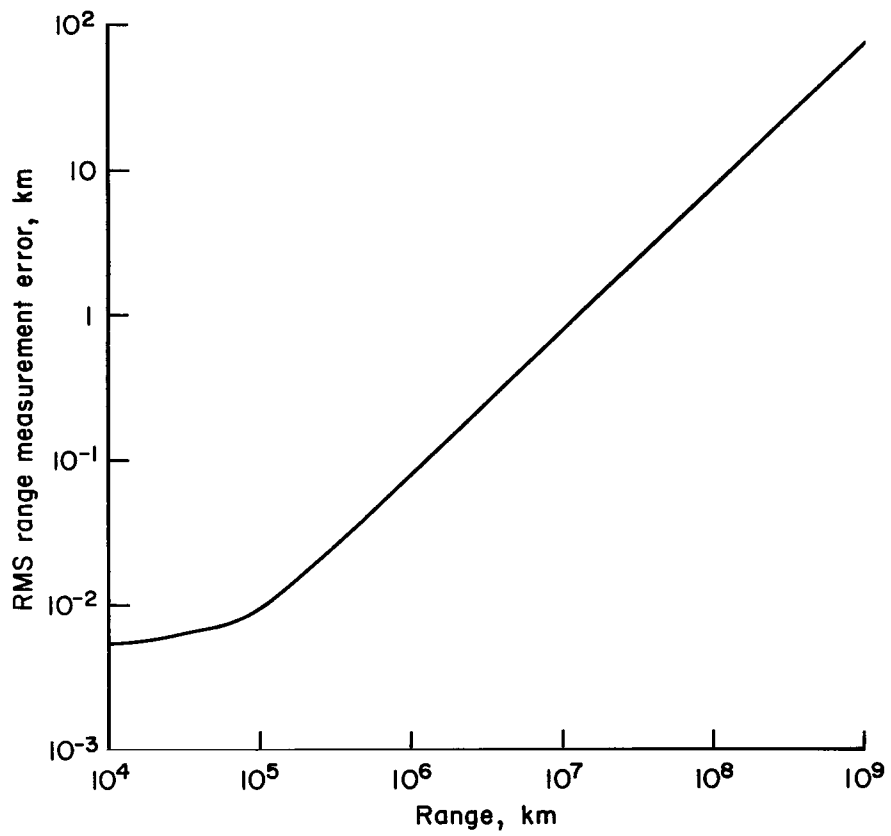


Figure 1.- Radar range measurement error.

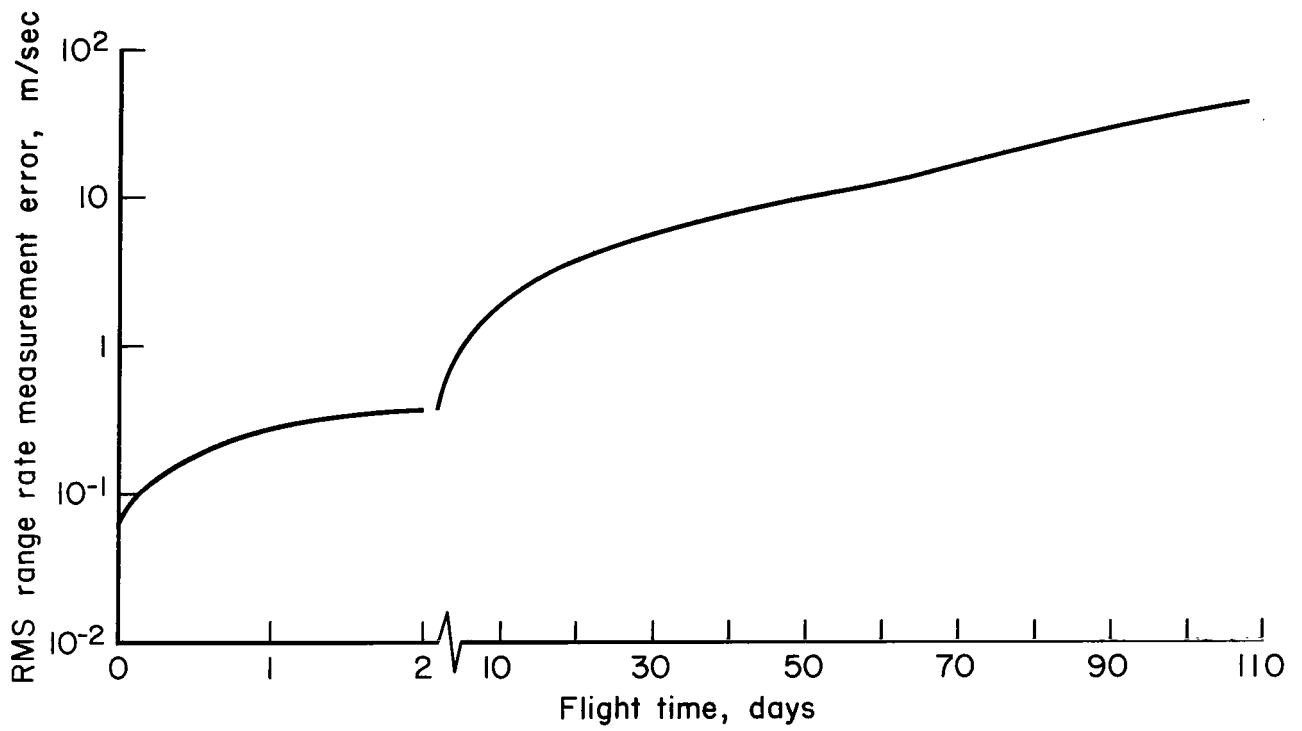
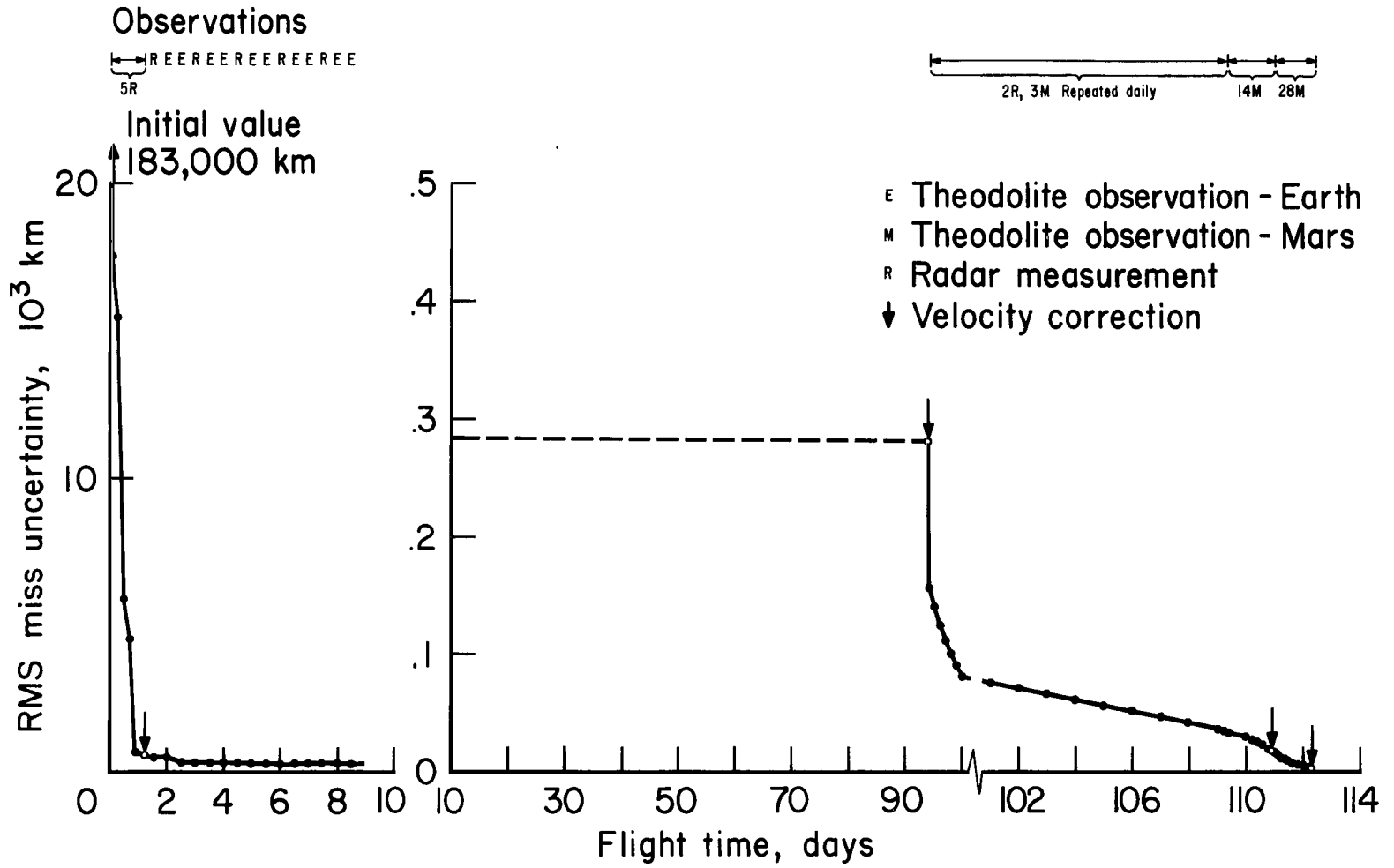
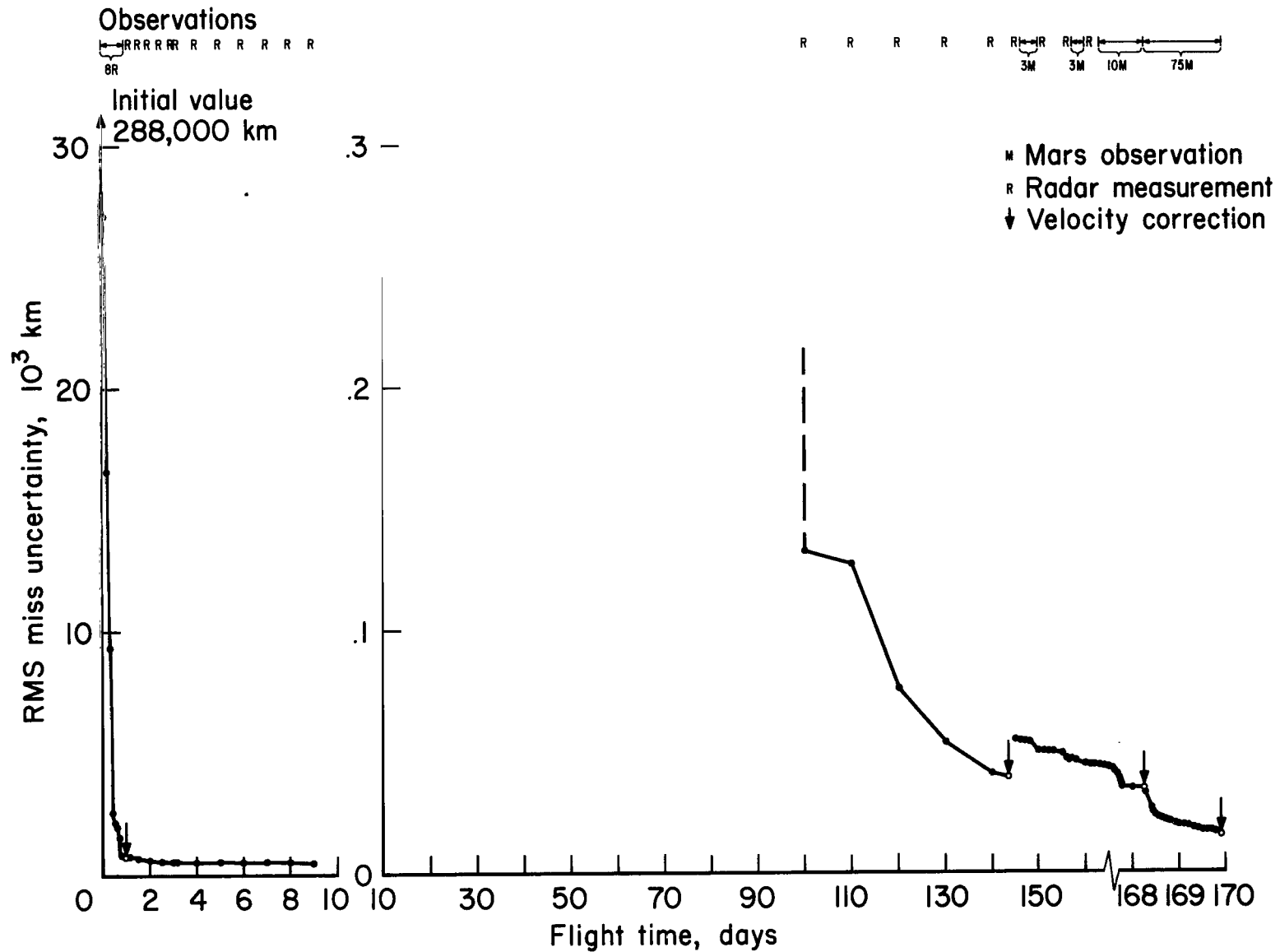


Figure 2.- RMS range-rate measurement error, high-speed mission, outbound leg.



(a) Outbound leg

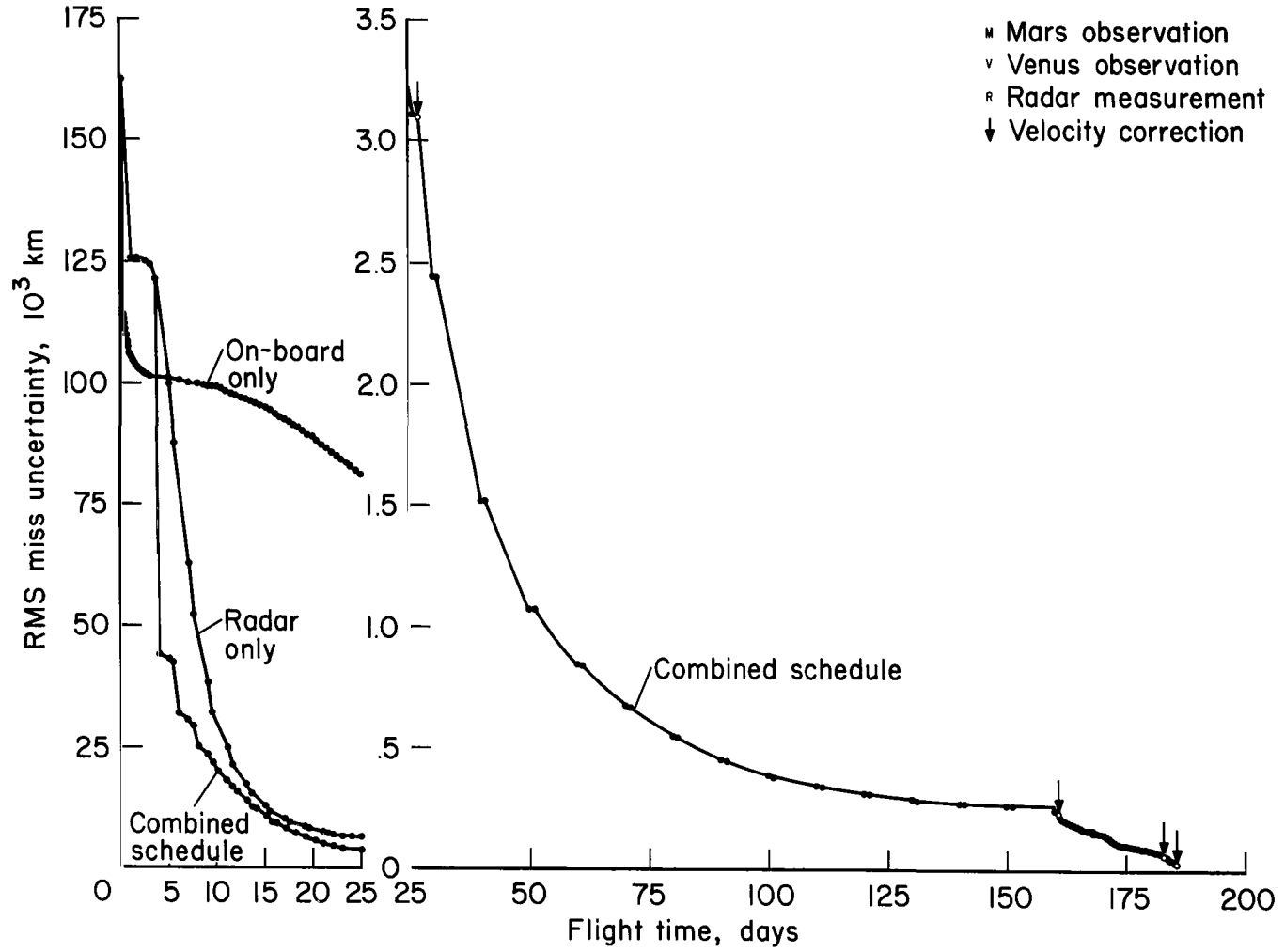
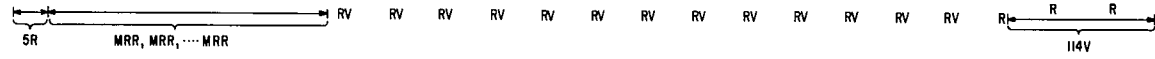
Figure 3.- RMS miss estimate error - high-speed mission.



(a) Outbound leg

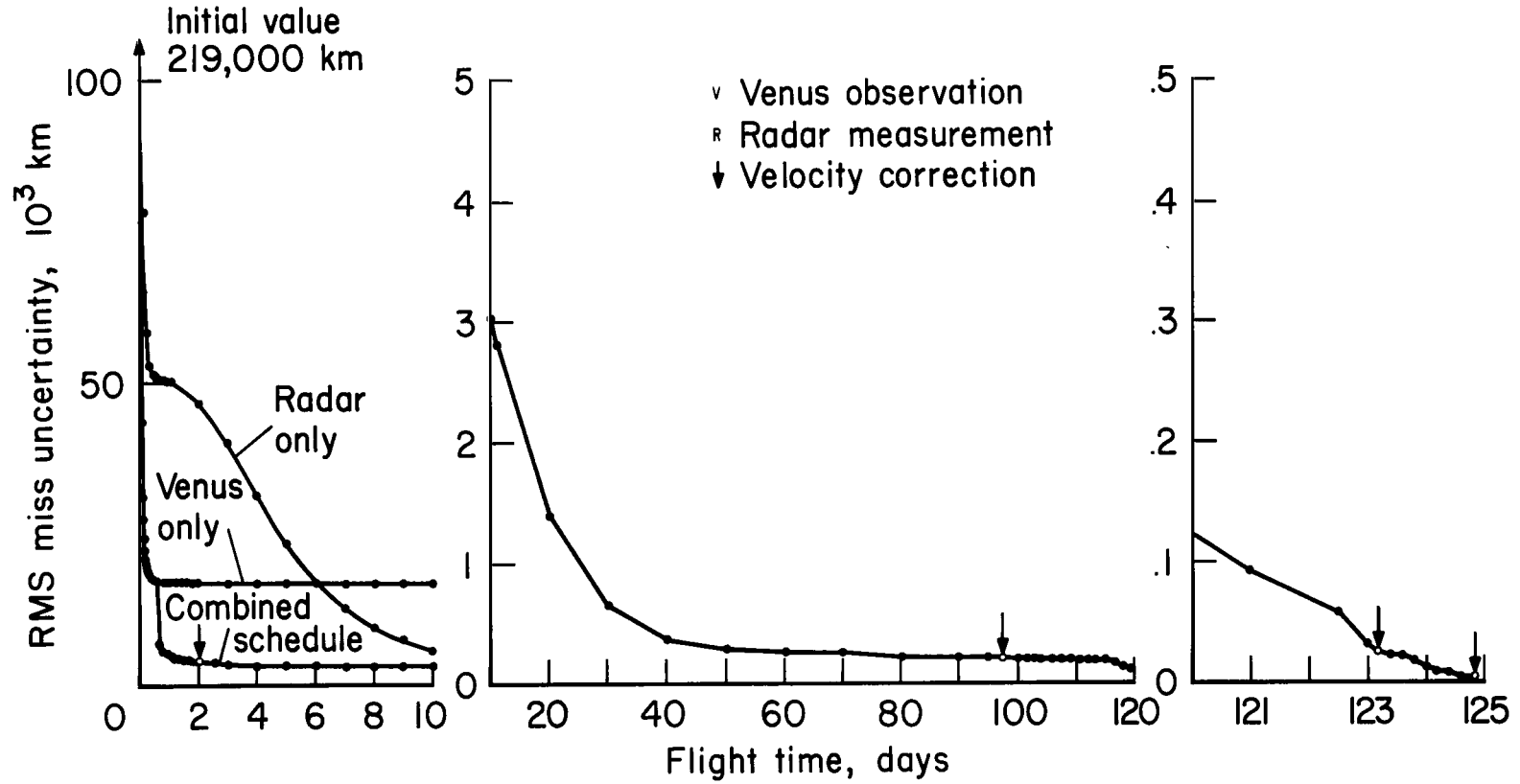
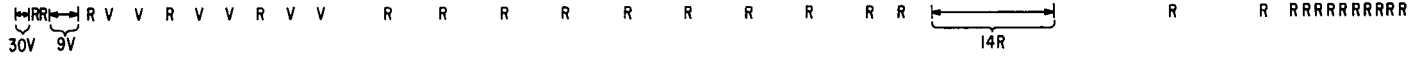
Figure 4.- RMS miss estimate error, Venus swing-by mission.

Observations



(b) Mars-Venus leg
 Figure 4.- Continued.

Observations



(c) Venus-Earth leg
Figure 4.- Concluded.

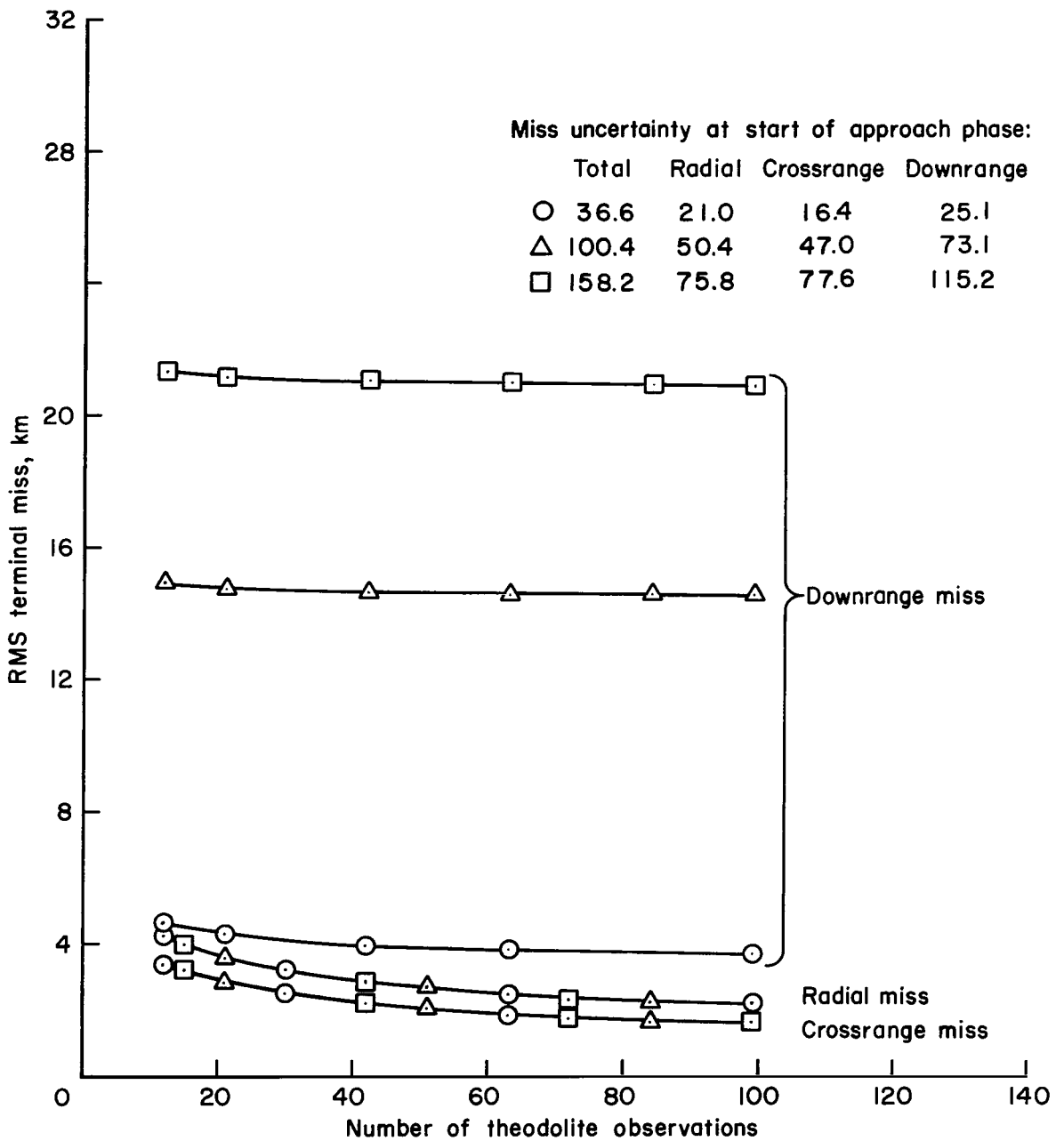


Figure 5.- Miss performance variation with approach phase schedule, high-speed mission, outbound leg.

Schedules

Radar-only

RRRRRR RR RR RR RR RR RR RR RR RRR R R R R R R R R

Combined

RRRRRRM RRM RRM RRM RRM RRM RRM RRM RRM RRM RR^M M R M R M R M R

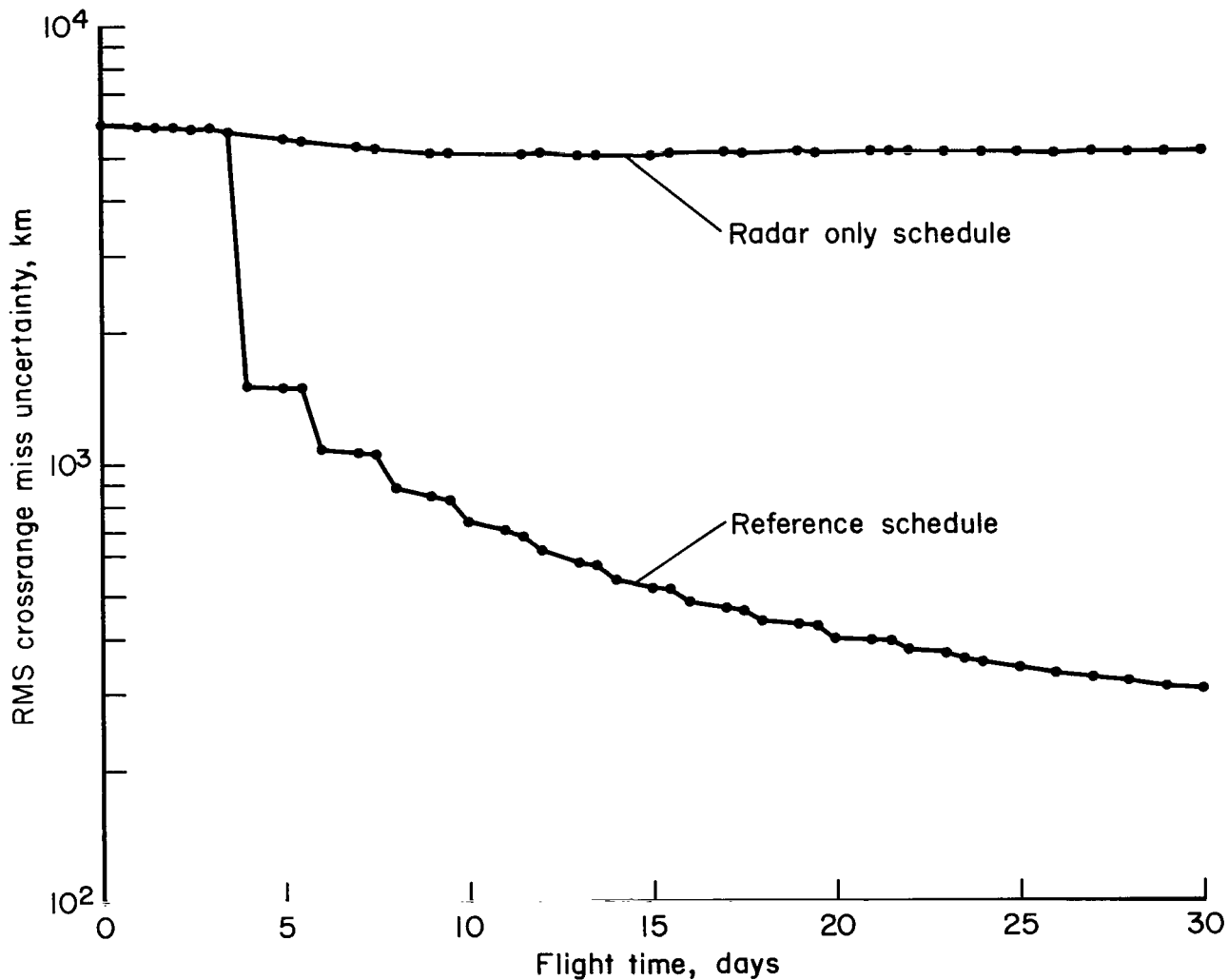


Figure 6.- Mars-Venus leg, effect of Mars observations on crossrange miss uncertainty.

"The aeronautical and space activities of the United States shall be conducted so as to contribute . . . to the expansion of human knowledge of phenomena in the atmosphere and space. The Administration shall provide for the widest practicable and appropriate dissemination of information concerning its activities and the results thereof."

—NATIONAL AERONAUTICS AND SPACE ACT OF 1958

NASA SCIENTIFIC AND TECHNICAL PUBLICATIONS

TECHNICAL REPORTS: Scientific and technical information considered important, complete, and a lasting contribution to existing knowledge.

TECHNICAL NOTES: Information less broad in scope but nevertheless of importance as a contribution to existing knowledge.

TECHNICAL MEMORANDUMS: Information receiving limited distribution because of preliminary data, security classification, or other reasons.

CONTRACTOR REPORTS: Technical information generated in connection with a NASA contract or grant and released under NASA auspices.

TECHNICAL TRANSLATIONS: Information published in a foreign language considered to merit NASA distribution in English.

TECHNICAL REPRINTS: Information derived from NASA activities and initially published in the form of journal articles.

SPECIAL PUBLICATIONS: Information derived from or of value to NASA activities but not necessarily reporting the results of individual NASA-programmed scientific efforts. Publications include conference proceedings, monographs, data compilations, handbooks, sourcebooks, and special bibliographies.

Details on the availability of these publications may be obtained from:

SCIENTIFIC AND TECHNICAL INFORMATION DIVISION
NATIONAL AERONAUTICS AND SPACE ADMINISTRATION
Washington, D.C. 20546